IMAGE-LIDAR INTERACTIVE VISUALIZATION ENVIRONMENT (I-LIVE) FOR MOBILE MAPPING SYSTEMS

Radhika Ravi [1, *], Ayman Habib [1]

[1] Lyles School of Civil Engineering, Purdue University, West Lafayette, IN, USA - (ravi22, ahabib)@purdue.edu

KEY WORDS: Mobile Mapping Systems, Imaging Systems, LiDAR, System Calibration, Visualization, Trajectory Evaluation, Applications

ABSTRACT:

Mobile Mapping Systems (MMS) equipped with laser scanners and cameras have been proven as a feasible tool for a plethora of surveying applications due to their ability to rapidly collect data over areas such as agricultural fields, transportation corridors, accident scenes, and other areas which cannot be surveyed manually. Although each sensor onboard an MMS provides invaluable information, the key strength lies in the amalgamation of information derived from all the sensors together. The level of information gathered from a combination of sensors is dependent on two factors – 1) the accuracy of registration of data from the different sensors and therefore, the accuracy of system calibration, and 2) the ability to visualize registered data simultaneously from different sensors mounted on different platforms. In this paper, we present an interface named I-LIVE (or, Image-LiDAR Interactive Visualization Environment), which is primarily developed as a tool aimed for end-users to conduct a qualitative and quantitative evaluation of data acquired from any UAV-based or wheel-based MMS. The major contribution of I-LIVE is the integration of data acquired in the form of point clouds (3D) and images (2D), in order to analyze the quality of GNSS/INS-derived trajectory and LiDAR-camera system calibration. Apart from the basic tools to integrate the 2D and 3D modalities for qualitative and quantitative quality control of the acquired data, I-LIVE also facilitates other application-specific tools for data visualization and information extraction, such as crop monitoring for agricultural applications and highway work zone monitoring for transportation applications. With such functionalities, I-LIVE is one of the first tools to equip the end-users for an effective data analysis and information extraction across all domains that rely on information from multiple sensors, such as LiDAR units and cameras, onboard mobile platforms.

1. INTRODUCTION

Mobile mapping systems equipped with laser scanners and cameras are becoming a widespread tool for a plethora of surveying applications, such as digital building model generation, transportation corridor monitoring, telecommunications, precision agriculture, infrastructure monitoring, and power line clearance evaluation [1], [2], [3], [4]. With this hike in demand for mobile mapping, calibration of such systems equipped with different sensors has become an active topic of research. Over the past few years, extensive research has been conducted for the calibration of airborne and terrestrial mobile mapping systems consisting of laser scanners [5], [6], [7]. Habib et al. [8] studied the impact of airborne LiDAR system calibration on the relative and absolute accuracy of the derived point clouds, both qualitatively and quantitatively. The relative accuracy was evaluated by quantifying the degree of co-alignment of overlapping strips before and after calibration, whereas the absolute accuracy was evaluated by quantifying the degree of compatibility between LiDAR and control surfaces before and after calibration. Muhammad et al. [9] performed calibration of a rotating multi-beam LiDAR with the objective to align the scan data as close as possible to a ground truth environment. He et al. [10] used pairwise multi-type 3D geometric features (i.e., point, line, plane) to derive the extrinsic parameters between 2D LiDAR and GPS/IMU. Similarly, several techniques have been developed to accurately calibrate different types of cameras in order to obtain accurate estimates of their intrinsic and extrinsic parameters. Weng et al. [11] proposed a two-step stereo camera calibration procedure to obtain the intrinsic parameters and the exterior orientation parameters of the involved cameras. The first step aims at obtaining the calibration parameters using a closed-form solution by assuming a distortion-free camera model. Then, the parameters obtained in the first step are improved iteratively through a non-linear optimization, taking into account camera distortions. Zhang et al. [12] proposed a technique for camera calibration using a planar pattern captured by a camera from different orientations. While such extensive research has been conducted in the field of calibration of systems consisting of LiDAR units and/or cameras [13], [14], [15], [16], [17], none of these works address the issue of conducting a quality control strategy for acquired data after calibration, especially for end-users who would proceed with data processing under the assumption that the data satisfies their accuracy requirement. So, in this paper, we present a user-interface denoted henceforth as I-LIVE (or, Image-LiDAR Interactive Visualization Environment) to aid end-users in conducting a qualitative evaluation of data acquired from any UAV-based or wheel-based MMS. I-LIVE consists of two types of viewers – Point Cloud Viewer (PCV) and Image Viewer (IV). PCV allows a simultaneous visualization of 3D point clouds acquired over different dates by all the LiDAR units onboard different mobile platforms. At the same time, IV allows the streaming of images captured by all the time-synchronized cameras aboard the MMS. One should note that a key feature of I-LIVE is its ability to display 3D point clouds or 2D imagery data simultaneously for datasets captured over different dates, from different sensors, and from different mobile platforms. Each stream of images captured by synchronized cameras over a data collection site can be loaded in a new instance of IV within I-LIVE to integrate them with the loaded data from other

* Corresponding author

modalities. The major contribution of I-LIVE is the integration of data acquired in the form of point clouds (3D) and images (2D), in order to analyze the quality of GNSS/INS-derived trajectory and LiDAR-camera system calibration. This quality assessment can be conducted in two different ways within I-LIVE:

1. **Images to Point Cloud:** I-LIVE allows to derive object space (3D) coordinates of any point observed in two or more distinct images either captured at different epochs and/or from different cameras at the same/different epochs. The derived 3D point is also displayed in PCV in order to show its alignment with respect to the acquired LiDAR-based point cloud.
2. **Point Cloud to Images:** On clicking a 3D point in PCV, the point is automatically backprojected onto the closest image(s) that captured the point. The point is displayed onto each of the images as one streams through the images captured at consecutive epochs. Also, it reports the additional images captured by the MMS that include the same point. Note that the quality of backprojection of a point across a sequence of images would indicate the accuracy level of system calibration and the quality of GNSS/INS-derived trajectory information.

Apart from the basic tools to integrate 2D and 3D modalities for quality control of GNSS/INS-derived trajectory and LiDAR-camera system calibration, I-LIVE also facilitates other application-specific tools for data visualization and information extraction, such as:

1. **Agricultural Applications:** Various agricultural fields are surveyed using UAVs and high-clearance tractors equipped with LiDAR units and cameras. I-LIVE is equipped with the ability to simultaneously display and integrate the point clouds and images acquired by different platforms on different dates for crop monitoring. Moreover, it allows the user to overlay the crop row/plot boundaries over 3D as well as 2D data.
2. **Transportation Applications:** Surveying and monitoring highways is a crucial task for road safety inspection and traffic accident reduction, especially in work zones. One of the key aspects used to facilitate a reduction in traffic congestion and accidents is ensuring that the lanes comply with the standard lane width requirement over highways and that the work zone alterations do not result in ambiguous lane markings. In this regard, I-LIVE demonstrates the ability to navigate through all such regions of interest (in PCV and IV) that are identified to either have narrow lanes or ambiguous lane markings. The regions are reported in I-LIVE while also displaying the extracted lane markings and a lane width scale bar (upto 12 ft) overlayed on images to provide a visual estimate of the actual lane width in the corresponding region. One should note that this feature would also enhance the ability for temporal monitoring of highways, especially in work zones where lane markings are constantly altered during the lifetime of a project. This alteration process could result in ambiguous lane markings or narrow lanes.

With such functionalities, I-LIVE is targeted to equip end-users with an effective data analysis and information extraction tool across all domains that rely on information from multiple sensors, such as LiDAR units and cameras, onboard mobile platforms.

2. MOBILE MAPPING SYSTEMS (MMS) USED IN THIS RESEARCH

The functionalities of the interface, I-LIVE, are demonstrated in this paper using data acquired from three different mobile mapping platforms – a wheel-based MMS (denoted henceforth as Purdue Wheel-based Mobile Mapping System, or PWMMS), an Unmanned Aerial Vehicle (UAV), and a high clearance tractor (denoted henceforth as PhenoRover). The wheel-based MMS, as shown in Figure 1, is mainly used for transportation applications and it consists of a Velodyne VLP-16 laser scanner, three Velodyne HDL-32E laser scanners, 3 Grasshopper cameras (two forward-viewing and one rear-viewing), and Applanix POSLV 220 GNSS/INS. The Applanix POSLV 220 combines GNSS and Inertial Measurement Unit (IMU) to provide accurate position and orientation information of the vehicle. The Grasshopper cameras are used as auxiliary sensors in this study and directly georeferenced by the POSLV 220 unit. The Grasshopper cameras have a maximum image resolution of 9.1 MP and all the cameras are synchronized to capture images at a rate of 1 frame per second per camera.

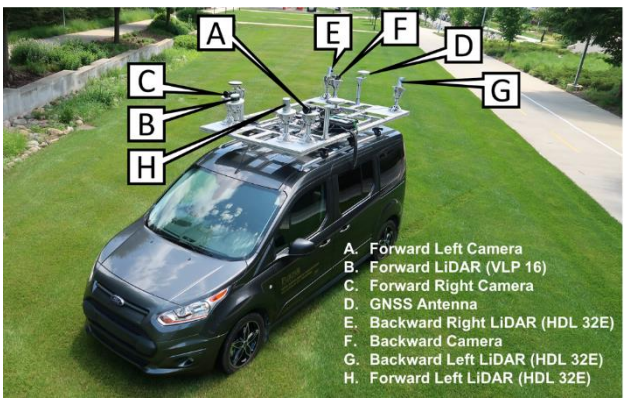

Figure 1. The wheel-based mobile mapping system (PWMMS) used in this research

The UAV-based system is mainly used for agricultural applications and it is developed using a DJI M600 as the platform to mount the LiDAR unit and RGB camera. Figure 2 shows the integrated UAV platform along with the mounted sensors. The system consists of a Velodyne VLP-16 Puck Hi-Res LiDAR unit and a Sony Alpha 7R RGB camera along with an Applanix APX-15 v3 GNSS/INS unit for direct georeferencing. The Velodyne VLP-16 Puck Hi-Res LiDAR unit has a typical range accuracy of 3 cm. The Sony Alpha 7R camera is a 36.4 MP off-the-shelf camera. This selection supports the goal of having maximum image resolution to facilitate accurate orthophoto generation and 3D point cloud reconstruction. For the APX-15 unit, the post-processing accuracy in position is 2 to 5 cm and the predicted accuracy for the roll/pitch and heading is 0.025 and 0.08˚, respectively [18].

The PhenoRover-based mobile mapping system, as shown in Figure 3, is used to collect close-range data for high-throughput phenotyping. The mobile mapping system onboard the PhenoRover consists of two Velodyne HDL-32E laser scanners and two Flea firewire cameras, which are directly georeferenced by an Applanix POSLV-125 unit. For the POSLV-125, the post-processing accuracy in position can be 2-5 cm and the achieved accuracy for the roll/pitch and heading can be 0.025˚ and 0.06˚, respectively [19]. The Flea cameras have an image resolution of 5 MP and both the cameras are synchronized to capture images at a rate of 1 frame per second per camera.

Figure 2. The UAV-based mobile mapping system used in this research

Figure 3. The PhenoRover-based mobile mapping system used in this research

3. MATHEMATICAL MODELS FOR POINT POSITIONING

Since this research introduces an environment for the integration of 2D and 3D data modalities, this section starts by introducing the point positioning equations for deriving the 3D mapping frame coordinates for points captured by LiDAR units and RGB cameras.

3.1 RGB Frame Cameras

A typical GNSS/INS-assisted frame camera system would involve 3 coordinate systems (i.e., mapping frame, IMU body frame, and camera coordinate frame). A given point, ***I***, captured in an image as point, ***i***, from a camera onboard a mobile mapping system can be reconstructed in the mapping coordinate system using Equation 1. Here, $r_i^C(t)$ denotes the distortion-free coordinates of a point, ***i***, in an image captured by camera, C, relative to the camera coordinate system. The camera (C) is related to the IMU body frame by a rigidly defined lever arm, r_C^b, and boresight matrix, R_C^b. Finally, each point, ***i***, in an image captured by camera, C, at time, t, has a scaling factor associated with it, which is denoted by $\lambda(i, C, t)$. The GNSS/INS integration provides the time dependent position, $r_b^m(t)$, and rotation, $R_b^m(t)$, relating the mapping frame and IMU body frame coordinate systems, according to the optimized solution from the available GNSS and inertial measurements. The lever arm, r_C^b, and the boresight angles constituting R_C^b, are derived from system calibration.

$$r_I^m = r_b^m(t) + R_b^m(t)\, r_C^b + \lambda(i, C, t)\, R_b^m(t)\, R_C^b\, r_i^C(t) \qquad (1)$$

3.2 LiDAR Unit

A typical LiDAR system would involve 3 coordinate systems (i.e., mapping frame, IMU body frame, and laser unit frame). A given point, ***I***, acquired from a mobile mapping system equipped with a laser scanner can be reconstructed in the mapping coordinate system using Equation 2. Here, $r_I^{lu}(t)$ denotes the coordinates of a 3D point relative to the laser unit coordinate system. The laser unit (lu) is related to the IMU body frame by a rigidly defined lever arm, r_{lu}^b, and boresight matrix, R_{lu}^b, which are derived from system calibration.

$$r_I^m = r_b^m(t) + R_b^m(t)\, r_{lu}^b + R_b^m(t)\, R_{lu}^b\, r_I^{lu}(t) \qquad (2)$$

Equations (1) and (2) are used further in this paper to establish point-to-point correspondences between the different modalities. One should note that the mobile mapping systems used in this research are calibrated using the approaches suggested in [20], [21], and [22] for LiDAR calibration and a simultaneous LiDAR-camera calibration for UAV-based and wheel-based mobile mapping systems.

4. QUALITY CONTROL USING I-LIVE

The integration of 2D and 3D data modalities in I-LIVE facilitates a point-to-point correspondence between the different modalities. These correspondences are derived as a function of the system calibration parameters along with the GNSS/INS-derived trajectory information, thus indicating their quality. The mapping of a point from 3D point cloud to imagery is achieved by conducting a backprojection of the 3D point onto the image space, i.e., using Equation (1) to derive $r_i^C(t)$. The derived 2D image space coordinates, $r_i^C(t)$, are computed using the camera mounting parameters with respect to the onboard GNSS/INS unit derived from the LiDAR-camera system calibration and also, the position and orientation of the vehicle as derived from the GNSS/INS-based trajectory. Thus, the quality of registration of the 3D point and its corresponding backprojected 2D image point would indicate the accuracy of estimated LiDAR and camera mounting parameters and the quality of GNSS/INS-derived trajectory. An example of backprojection for the PWMMS is shown in Figure 4 (a), where the 3D point cloud consists of lane marking points extracted from the original point cloud based on intensity. Here, a corner of a lane marker is selected in the LiDAR data and it is backprojected by I-LIVE onto the stereo-pair images (in magenta) captured by the two front-facing cameras onboard the PWMMS. One should note that the image pair chosen by I-LIVE for display of the backprojection is one that captures the 3D point of interest from the closest position. However, a list of image IDs, as shown in Figure 4(a), is also displayed in I-LIVE indicating other images that also capture the point of interest. Similarly, an example of backprojection for the UAV-based MMS is shown in Figure 4 (b), where the LiDAR data displays a row of plants colored by height and a point on one of the plants is selected as the point of interest. This point is then backprojected by I-LIVE onto the RGB imagery that captures the point from the closest location and it is displayed in magenta.

(a)

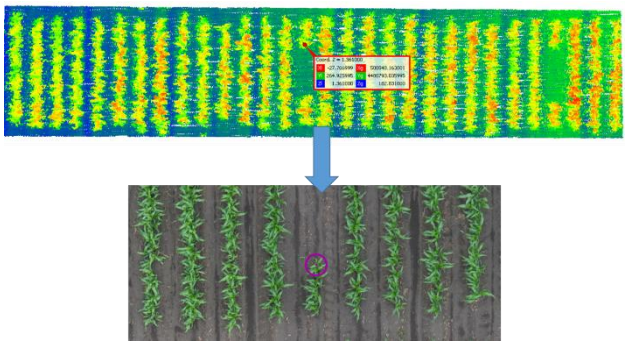

(b)

Figure 4. 3D to 2D Backprojection: (a) Lane markings (colored by intensity) from PWMMS and the backprojection of selected point on stereo-pair images (in magenta), (b) Row of plants (colored by height) from UAV-based MMS and the backprojection of selected point on UAV-based image

Similarly, I-LIVE allows the projection from 2D image space to 3D object space by conducting an intersection of light rays corresponding to the same point measured in different images captured either at different epochs and/or by different cameras. The derived 3D object point corresponding to the observed image points is then overlaid along with the existing point clouds loaded in the Point Cloud Viewer. An example of projection from 2D to 3D space is demonstrated for each of the three MMS (PWMMS, UAV-based, and PhenoRover-based) in Figure 5. Here, the observed image points for a point are marked in red in the RGB imagery and the corresponding derived 3D point is shown with its label overlaid on the existing LiDAR point cloud colored by intensity for each of the three MMS.

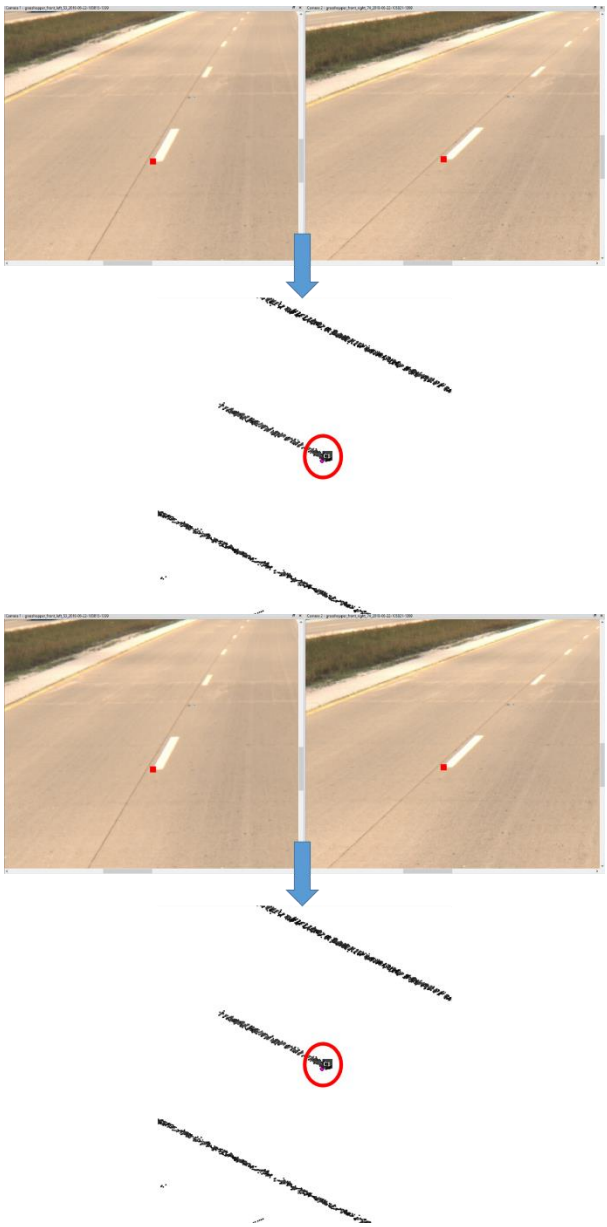

(a)

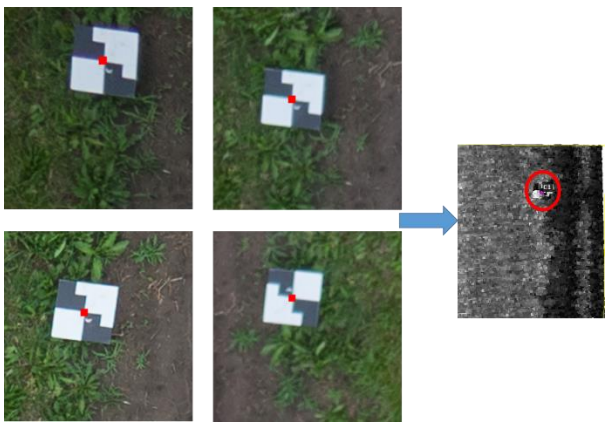

(b)

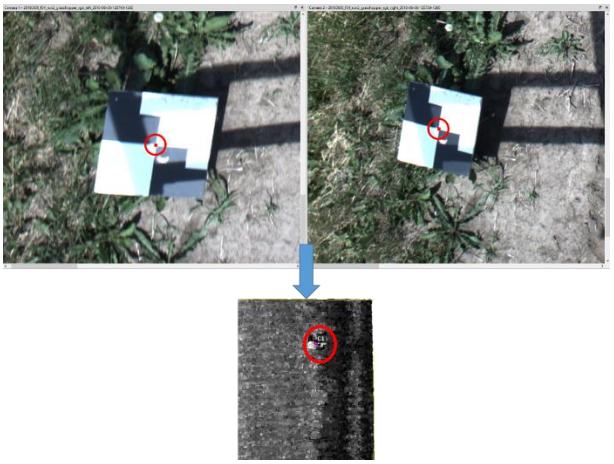

(c)

Figure 5. 2D to 3D Multiple Light Ray Intersection: (a) Corner of lane marking observed in a stereo-pair captured by different cameras at the same epoch from PWMMS, (b) Center of target measured in four images at different epochs from UAV-based MMS, (c) Center of target measured in a stereo-pair from PhenoRover-based MMS

In Figures 4 and 5, the correct location of the resultant 2D point from backprojection and 3D point from multiple light ray intersection with respect to the surrounding points validates the GNSS/INS-derived trajectory information and the accuracy of the estimated sensor mounting parameters from system calibration for the different mobile mapping platforms. The registration quality also validates the accuracy of the estimated interior orientation parameters (IOPs) of each of the cameras involved, such as the focal length, principal point location, and the distortion parameters.

5. APPLICATION-SPECIFIC I-LIVE FUNCTIONALITIES

Apart from I-LIVE serving as a tool for end-users to conduct a quality control of acquired data, I-LIVE also has built-in functionalities in order to render the information that would hold relevance with respect to specific applications, such as transportation corridor monitoring or agricultural monitoring. The functionalities developed for each of these two fields of application are described in more detail in the forthcoming subsections.

5.1 Transportation Corridor Monitoring

Transportation corridor monitoring is imperative for road safety inspection and traffic accident reduction. The road characteristics are more critical in work zones since the complex array of signs, barrels, and lane changes result in an increased rate of crashes. Lane width is an important characteristic in work zones since an area with narrow lanes significantly reduces the roadway capacity and increases the occurrence of traffic accidents. A wheel-based MMS can be utilized to capture LiDAR and RGB imagery data over the work zone area. Then, the acquired LiDAR point cloud can be used to evaluate the lane width in highway work zones by extracting lane markings from the road surface point cloud based on the intensity [23]. Finally, the identified lane markings are analyzed to identify areas with ambiguous lane markings and the normal distance between adjacent lane markings can be computed in order to estimate the lane widths along the highway and identify areas with narrow lanes. The derived lane width information along with the identified areas with ambiguous lane markings or narrow lanes serve as input for I-LIVE in order to facilitate the navigation from one region of interest (ROI) to another along the highway. Each region of interest to be visualized in I-LIVE is stored as a list of four points from the point pairs marking the start and end of the region. The reported ROIs are visualized in I-LIVE in two different ways:

1. **3D Visualization**: First, the reported area is displayed as a polygon in red formed by connecting the point pairs denoting the start and end of the region of interest, as shown in Figure 6 (a) for a sample ROI. The polygon is then overlaid on the extracted high intensity potential lane markings and the derived interpolated centerline points.
2. **2D Visualization**: The ROI is also visualized for validation using the RGB images captured during the data collection at a rate of 1 frame per second by the onboard Grasshopper cameras. An image corresponding to the sample ROI is shown in Figure 6 (b) to demonstrate the 2D visualization of an ROI. Two lines – one joining the starting point pair (in yellow) and another joining the ending point pair of the ROI (in green) – are drawn on the corresponding images to indicate the span of a narrow lane or ambiguous lane marking area. The corresponding images are also marked with the lane marking centerline point pairs, that are used for lane width estimation, spaced at 20 cm. These points are backprojected onto the images using the calibrated camera IOPs and mounting parameters along with the vehicle position and orientation derived from the trajectory information. The centerline points are marked either in cyan or magenta color, depending on whether the point is derived directly from the lane marking or from the interpolation between lane markings, respectively. Lastly, there are lane width scale bars at 3 m intervals overlaid on the images by joining the backprojections of the centerline point pairs in order to facilitate a visual inspection of the lane width. The scale bar is color-coded with a red portion extending from 0 to 9 ft, followed by a green portion upto 10 ft, yellow upto 11 ft, and blue till 12 ft.

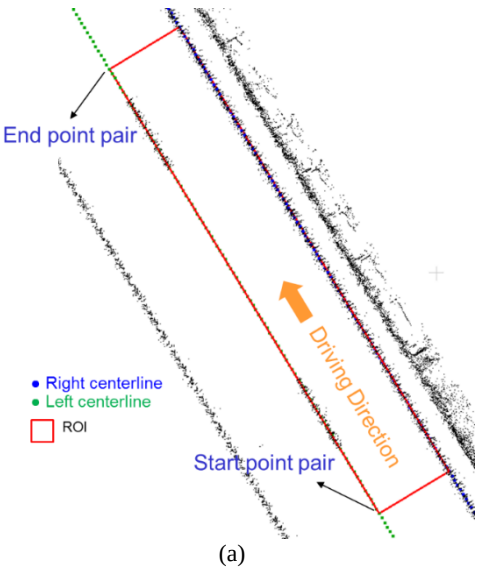

(a)

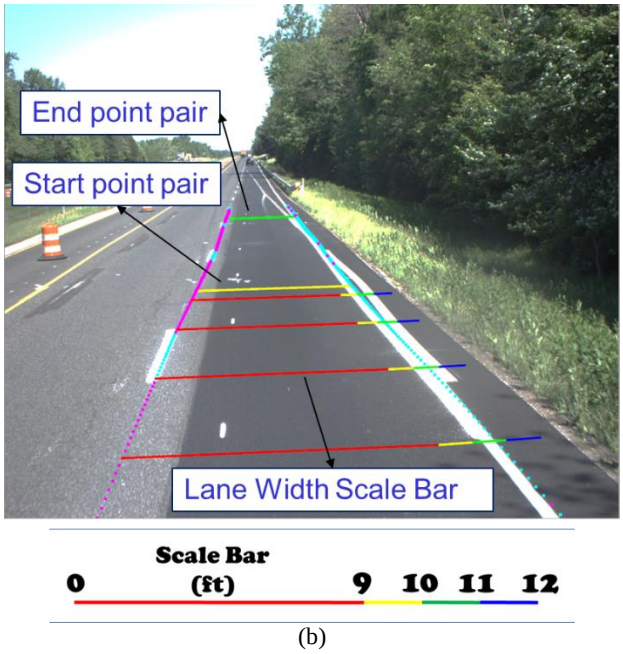

(b)

Figure 6. ROI Visualization: (a) 3D: ROI polygon overlaid on high intensity lane markings, (b) 2D: lane marking centerline points and ROI boundary overlaid on RGB imagery

5.2 Agricultural Applications

In this subsection, we introduce the functionalities of I-LIVE pertaining to agricultural applications, especially for high throughput phenotyping. As illustrated earlier, the 2D and 3D data acquired by a mobile mapping system is integrated in I-LIVE using the system calibration parameters and trajectory information. Agricultural fields are often surveyed with the purpose of crop growth monitoring, which requires data collection over the entire growing season at an interval of every few days. Here, we demonstrate the ability of I-LIVE to integrate data acquired over different dates from different sensors mounted on different platforms. Such an integration facilitates a time-series crop characteristic determination, which in turn facilitates a vast input data generation for models to predict valuable information, such as crop biomass, for studying and comparing different genotypes of the same crop. Such an integration of data from different modalities would reduce the need for a destructive sampling of crops for applications such as biomass prediction. The point cloud viewer and image viewer in I-LIVE show the growth of a crop at a specific location as viewed in LiDAR, Figure 7 (a), and RGB image data acquired by UAV, Figure 7 (b), and PhenoRover, Figure 7 (c), over different dates. An additional feature in I-LIVE is the ability to plot the row boundary for a selected plant point, which would further aid in identifying the genotype of the crop that the plant belongs to. This is overlaid on the image as a blue rectangle, as shown in Figures 7 (b) and (c). The integration of data from different dates and from different mobile platforms allows the monitoring of crop growth at a particular location. For instance, from Figures 7 (b) and (c), it can be seen that a set of plants around the selected point are visible in the PhenoRover images from 6th June but not visible in the UAV-based images from 11th June, which is caused by an intermediate destructive sampling conducted between 6th and 11th June.

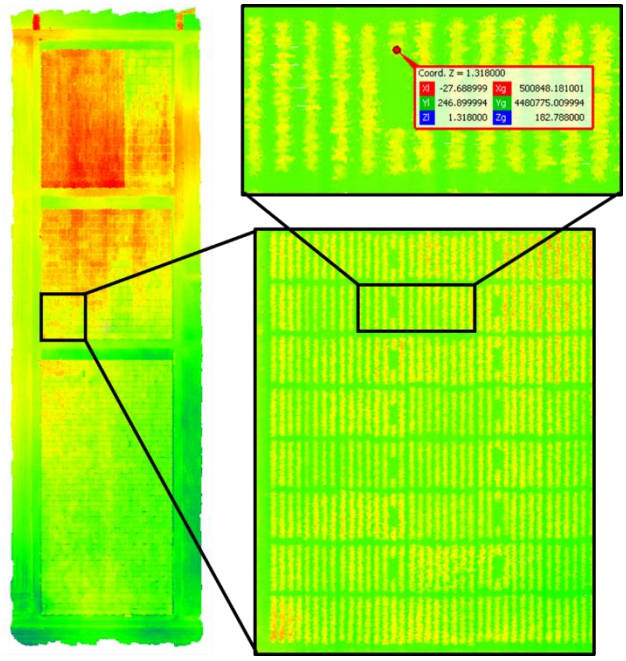

(a)

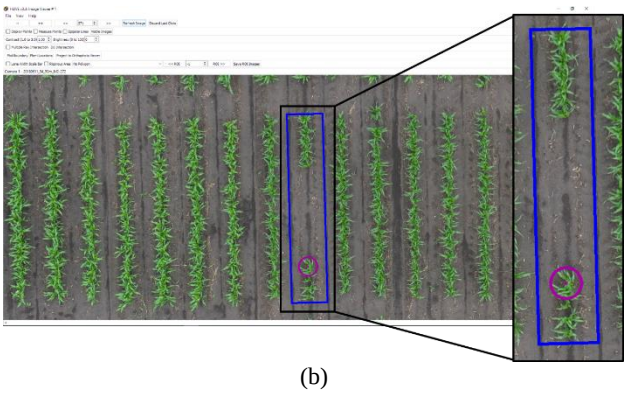

(b)

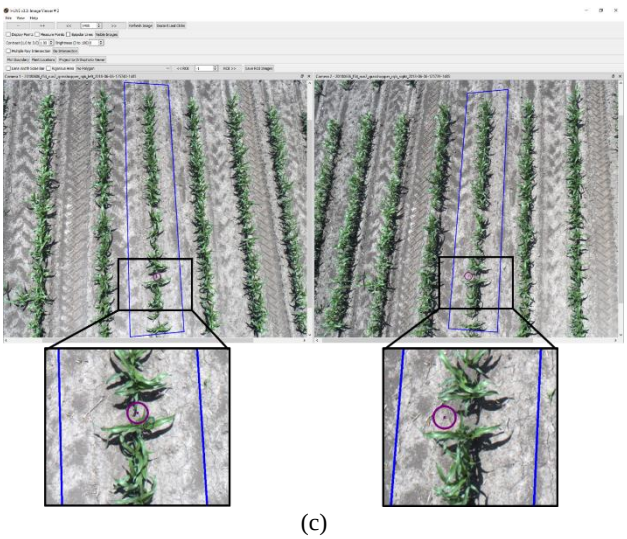

(c)

Figure 7. I-LIVE for Agriculture: (a) UAV-based LiDAR data from 11th June, (b) UAV-based RGB Imagery from 11th June, and (c) PhenoRover-based Stereo-pair of images from 6th June

Currently, we are expanding the functionalities of I-LIVE to display and integrate RGB orthophotos in order to facilitate its use as a tool for training data acquisition for deep learning and machine learning networks that are trained to non-destructively predict crop biomass. One of the key inputs to such networks is the plant center locations over the agricultural plot that are usually manually measured using RGB orthophotos. However, as the crops grow, it becomes difficult to delineate one plant location from another. Here, the ability of I-LIVE to integrate the orthophoto with close-range images captured by PhenoRover-based MMS on early dates in the growing season would help in the decision-making process and ensure an accurate training data collection for the prediction models.

6. CONCLUSIONS AND RECOMMENDATIONS FOR FUTURE WORK

This paper presented an interactive visualization environment (I-LIVE) that can integrate LiDAR and image data acquired by different platforms at different dates over the same area simultaneously in order to facilitate an efficient monitoring of assets in different domains. With in-built functions for image streaming, image measurement, backprojection, and light ray intersection, I-LIVE is one of the first tools aimed at providing the end-users with the ability to perform a quality check of the acquired data and to evaluate the quality of registration of data from different sensor modalities. The application-specific functionalities of I-LIVE are currently focusing on agricultural and transportation engineering, but we aim to add further functionalities pertaining to infrastructure monitoring and shoreline monitoring in order to serve a larger group of end-users. In the future, we also hope to add the support for other sensor types, such as hyperspectral push-broom scanners, and introduce a new component for orthophoto visualization and manipulation integrated with the point cloud and image viewers. Apart from enhancing application-specific functionalities, we also aim to add tools in I-LIVE for increasing the level of automation of system calibration by allowing an automatic intensity-based or geometry-based planar and linear feature extraction from 3D point clouds.

ACKNOWLEDGEMENTS (OPTIONAL)

This work was supported in part by the Joint Transportation Research Program – administered by the Indiana Department of Transportation and Purdue University – and the Advanced Research Projects Agency-Energy (ARPA-E), U.S. Department of Energy, under Award Number DE-AR0000593. The contents of this paper reflect the views of the authors, who are responsible for the facts and the accuracy of the data presented herein, and do not necessarily reflect the official views or policies of the sponsoring organizations.

REFERENCES

1. Lin, Hui, et al. "Semantic decomposition and reconstruction of residential scenes from LiDAR data." *ACM Transactions on Graphics (TOG)* 32.4 (2013): 66.
2. Williams, Keith, et al. "Synthesis of transportation applications of mobile LiDAR." *Remote Sensing* 5.9 (2013): 4652-4692.
3. Weiss, Ulrich, and Peter Biber. "Plant detection and mapping for agricultural robots using a 3D LIDAR sensor." *Robotics and autonomous systems* 59.5 (2011): 265-273.
4. Puente, I., et al. "Review of mobile mapping and surveying technologies." *Measurement* 46.7 (2013): 2127-2145.
5. Chan, T., Derek D. Lichti, and David Belton. "Temporal analysis and automatic calibration of the velodyne hdl-32e lidar system." *ISPRS Ann. Photogramm. Remote Sens. Spat. Inf. Sci* 2 (2013): 61-66.
6. Atanacio-Jiménez, Gerardo, et al. "Lidar velodyne hdl-64e calibration using pattern planes." *International Journal of Advanced Robotic Systems* 8.5 (2011): 59
7. Glennie, C. L., A. Kusari, and A. Facchin. "Calibration and stability analysis of the vlp-16 laser scanner." *The International Archives of Photogrammetry, Remote Sensing and Spatial Information Sciences* 40 (2016): 55
8. Habib, Ayman F., et al. "Geometric calibration and radiometric correction of LiDAR data and their impact on the quality of derived products." *Sensors* 11.9 (2011): 9069-9097.
9. N. Muhammad and S. Lacroix, “Calibration of a rotating multi-beam lidar,” in *Intelligent Robots and Systems (IROS), 2010 IEEE/RSJ International Conference on*, 2010, pp. 5648–5653.
10. M. He, H. Zhao, F. Davoine, J. Cui, and H. Zha, “Pairwise LIDAR calibration using multi-type 3D geometric features in natural scene,” in *Intelligent Robots and Systems (IROS), 2013 IEEE/RSJ International Conference on*, 2013, pp. 1828–1835.
11. Weng, Juyang, Paul Cohen, and Marc Herniou. "Camera calibration with distortion models and accuracy evaluation." *IEEE Transactions on pattern analysis and machine intelligence* 14.10 (1992): 965-980.
12. Zhang, Zhengyou. "A flexible new technique for camera calibration." *IEEE Transactions on pattern analysis and machine intelligence* 22.11 (2000): 1330-1334.
13. A. R. Willis, M. J. Zapata, and J. M. Conrad, “A linear method for calibrating LIDAR-and-camera systems,” in Modeling, Analysis & Simulation of Computer and Telecommunication Systems, 2009. MASCOTS’09. IEEE International Symposium on, 2009, pp. 1–3.
14. L. Zhou and Z. Deng, “Extrinsic calibration of a camera and a lidar based on decoupling the rotation from the translation,” in Intelligent Vehicles Symposium (IV), 2012 IEEE, 2012, pp. 642–648.
15. G. Pandey, J. R. McBride, S. Savarese, and R. M. Eustice, “Automatic Targetless Extrinsic Calibration of a 3D Lidar and Camera by Maximizing Mutual Information.,” in AAAI, 2012.
16. S. Bileschi, “Fully automatic calibration of lidar and video streams from a vehicle,” in Computer Vision Workshops (ICCV Workshops), 2009 IEEE 12th International Conference on, 2009, pp. 1457–1464.
17. X. Gong, Y. Lin, and J. Liu, “3D LIDAR-camera extrinsic calibration using an arbitrary trihedron,” Sensors, vol. 13, no. 2, pp. 1902–1918, 2013.
18. Applanix. APX-15 UAV Version 3, Single Board GNSS-Inertial Solution, https://www.applanix.com/downloads/products/specs/APX15_UAV.pdf (Accessed 03 Apr 2019).
19. Applanix. POSLV 125 Mobile Geospatial Data Acquisition: Designed for Integration, Built for Performance, https://www.applanix.com/pdf/POS_LV_125_Data_Sheet.pdf (Accessed 03 Apr 2019).
20. Ravi, R., Lin, Y. J., Elbahnasawy, M., Shamseldin, T., & Habib, A. (2018). Bias impact analysis and calibration of terrestrial mobile lidar system with several spinning multibeam laser scanners. *IEEE Transactions on Geoscience and Remote Sensing*, *56*(9), 5261-5275.
21. Ravi, R., Lin, Y. J., Elbahnasawy, M., Shamseldin, T., & Habib, A. (2018). Simultaneous System Calibration of a Multi-LiDAR Multicamera Mobile Mapping

Platform. *IEEE Journal of selected topics in applied earth observations and remote sensing*, *11*(5), 1694-1714.

22. Ravi, R., Shamseldin, T., Elbahnasawy, M., Lin, Y. J., & Habib, A. (2018). Bias Impact Analysis and Calibration of UAV-Based Mobile LiDAR System with Spinning Multi-Beam Laser Scanner. *Applied Sciences*, *8*(2), 297.
23. Habib, A., Lin, Y.-J., Ravi, R., Shamseldin, T., & Elbahnasawy, M. (2018). *LiDAR-based mobile mapping system for lane width estimation in work zones* (Joint Transportation Research Program Publication No. FHWA/IN/JTRP-2018/10). West Lafayette, IN: Purdue University.